

Figure S1: Numerical scheme to determine v_m . Each column (1-3) shows the temperature field (row a), temperature at the bed (row b) and net heat flux $k(\partial T/\partial z|^+ - \partial T/\partial z|^ -)$ into the bed (row c). Note that $k(\partial T/\partial z|^+ - \partial T/\partial z|^ -) = -\tau_c \sqrt{u^2 + v^2}$ for $y < 0$. Temperature contours are plotted in 5°C intervals, with $T = 0^\circ\text{C}$ marked with a bold red line. Column 1 shows results for $v_m = 0.70$ m/year and an apparently singular heat flux at the origin in panel c₁. Column 2 shows results for $v_m = 0.63$ m/year with constraint (17a)₁ violated in panel b₂. Column 3 shows results for $v_m = 0.65$ m/year, satisfying both constraints. Note that the results in rows b and c are plotted for a narrow range of y around the origin. The region in which the inequality constraints are violated can be quite small even for substantially incorrect values of v_m . This underlines the need for a high grid resolution around the origin in our computations. Calculations were done with the values listed in table 1 and $\tau_c = 5\tau_s = 1000$ kPa.

39 S2 Velocity, shear heating and temperature close to the cold-temperate 40 transition

41 Here we extend the analysis of shear heating and temperature fields in appendix A of Schoof (2012)
42 to the case of a transition from slip at a fixed basal yield stress τ_c to free stress. Our purpose is to
43 demonstrate mathematically that the temperature field near the origin (assumed to be the location at
44 which the cold-temperate transition takes place) allows only the three different cases described above:

- 45 1) positive temperatures for $y < 0$, conflicting with the assumption that the bed there is subtemperate,
46 and subtemperate sliding is taking place
- 47 2) an infinite heat flux out of the bed, corresponding to an infinite rate of basal freezing on the warm
48 side of the origin $y > 0$
- 49 3) as a limiting case, a finite rate of freezing on the warm side of the bed, equal to the dissipation
50 rate on the subtemperate side of the bed

51 The numerical scheme in the previous section S1 is built on the assumption that the limiting case 3
52 is the only physically acceptable one.

53 For simplicity, we restrict ourselves to the case of constant ice viscosity η , and consider only flow
54 parallel to the margin, assuming that the velocity component in the direction is much larger than the

55 transverse velocity and therefore dominates the shear heating rate. We can treat the velocity as being
 56 the sum of a constant sliding velocity \bar{u}_b at the transition from frictional to free slip, and a correction
 57 $\tilde{u}(y, z)$. The latter then satisfies the Stokes flow problem

$$\eta \nabla^2 \tilde{u} = 0$$

58 for $z > 0$, where ∇ is the gradient operator in the transverse y - z -plane, with boundary conditions

$$\eta \frac{\partial \tilde{u}}{\partial z} = \begin{cases} \tau_c & \text{at } z = 0, y < 0 \\ 0 & \text{at } z = 0, y > 0. \end{cases}$$

59 A general solution can be derived using complex variables, letting $\zeta = y + iz$, and using the differen-
 60 tiation rules (England, 1971)

$$\frac{\partial}{\partial y} = \frac{\partial}{\partial \zeta} + \frac{\partial}{\partial \bar{\zeta}} \quad \frac{\partial}{\partial z} = i \left(\frac{\partial}{\partial \zeta} - \frac{\partial}{\partial \bar{\zeta}} \right). \quad (\text{S1})$$

61 Since \tilde{u} satisfies Laplace's equation, it is the real part of a holomorphic function $\phi(\zeta)$, $\tilde{u}(y, z) =$
 62 $\text{Re}(\phi(\zeta))$, and we have $\partial \tilde{u} / \partial y + i \partial \tilde{u} / \partial z = \phi'(\zeta)$ (England, 1971). Continuing ϕ' analytically to the
 63 lower half-plane $\Im(\zeta) < 0$ by defining $\phi'(\zeta) = \phi'(\bar{\zeta})$ (note that ϕ' has no physical meaning in the lower
 64 half-plane), we find that the extended function ϕ' is analytic in the ζ -plane cut along the negative
 65 half of the real axis, where it satisfies $i(\phi'^+(y) - \phi'^-(y)) = 2\tau_c$. The superscripts $+$ and $-$ indicate
 66 limits taken from above and below, respectively. Hence an integrable solution takes the general form
 67 (Muskhelishvili, 1992)

$$\phi'(\zeta) = -\frac{\tau_c}{\pi\eta} \log(\zeta) + \sum_{n=0}^{\infty} c_n \zeta^n,$$

68 where \log is the usual branch of the natural logarithm with a branch cut on the negative real axis, and
 69 the c_n must be real to ensure the requisite symmetry of ϕ' . The corresponding velocity field expressed
 70 in polar coordinates, with $y = r \cos(\vartheta)$ and $z = r \sin(\vartheta)$, is

$$\tilde{u} = \frac{\tau_c}{\pi\eta} \{r\vartheta \sin(\vartheta) - r[\log(r) - 1] \cos(\vartheta)\} + \sum_{n=0}^n \frac{c_n}{n+1} r^{n+1} \cos[(n+1)\vartheta].$$

71 Next, we consider the heat transport problem. At short enough length scales, several simplifications
 72 can be made. To an error of $O(\text{Per})$, advection can be omitted, and the strain heating rate $\eta |\nabla \tilde{u}|^2$ can
 73 be approximated by retaining only the first two terms in the solution for $\phi' \sim -\tau_c / (\pi\eta) \log(\zeta) + c_0$. In
 74 computing frictional dissipation due to sliding at the bed, we can also approximate the sliding velocity
 75 by \bar{u}_b to an error of $O(r \log(r))$. Hence, to an error of that magnitude,

$$-k \nabla^2 T = \begin{cases} \frac{\tau_c^2}{\pi^2 \eta} [\log(r/r_0)^2 + \vartheta^2] & \text{for } z > 0, \\ 0 & \text{for } z < 0, \end{cases} \quad (\text{S2})$$

76 with the boundary conditions

$$T(y, 0) = 0 \quad \text{for } z = 0, y > 0, \quad (\text{S3})$$

$$-k \left[\frac{\partial T}{\partial z} \right]_{-}^{+} = \tau_c \bar{u}_b \quad \text{for } z = 0, y < 0, \quad (\text{S4})$$

$$[T(y, 0)]_{-}^{+} = 0 \quad \text{for } z = 0, y < 0 \quad (\text{S5})$$

77 where $\log(r_0) = c_0 \pi \eta / \tau_c$. Importantly, the heat production rate for the no-slip to free-slip transition
 78 in Schoof (2012) behaves as $1/r$, whereas it has only a logarithmic singularity in r here.

79 Using (S1), we can express Poisson's equation (S2) in terms of ζ as

$$-4k \frac{\partial^2 T}{\partial \zeta \partial \bar{\zeta}} = \begin{cases} \frac{\tau_c^2}{\pi^2 \eta} \log(\zeta/r_0) \log(\bar{\zeta}/r_0) & \text{for } \Im(\zeta) > 0 \\ 0 & \text{for } \Im(\zeta) < 0. \end{cases} \quad (\text{S6})$$

80 We can write the solution in the form

$$\begin{aligned}
T = & -\frac{\tau_c^2}{8\pi^2 k \eta} \left\{ 2 [\zeta \log(\zeta/r_0) - \zeta] [\bar{\zeta} \log(\bar{\zeta}/r_0) - \bar{\zeta}] \right. \\
& - [\zeta \log(\zeta/r_0) - \zeta]^2 - [\bar{\zeta} \log(\bar{\zeta}/r_0) - \bar{\zeta}]^2 \\
& + 2i\pi [\zeta^2 \log(\zeta/r_0) - \bar{\zeta}^2 \log(\bar{\zeta}/r_0) + \bar{\zeta}^2 - \zeta^2] + i\pi (\zeta^2 - \bar{\zeta}^2) \left. \right\} \\
& + i \frac{\tau_c \bar{u}_b}{2k} (\zeta - \bar{\zeta}) + \varphi(\zeta) + \overline{\varphi(\zeta)} \quad \text{for } \Im(\zeta) > 0 \\
T = & \varphi(\zeta) + \overline{\varphi(\zeta)} \quad \text{for } \Im(\zeta) < 0
\end{aligned}$$

81 where φ is an analytic function in the lower and upper half planes, its form to be determined by
82 the boundary conditions at the bed, where $\Im(\zeta) = 0$. Along the negative half of the real axis, the
83 boundary conditions (S4) and (S5) written in complex variable form using (S1) together ensure that
84 φ' and therefore φ are continuous across that boundary and hence analytic on the ζ -plane cut along
85 the positive real axis. On that branch cut, $\varphi^+(y) + \overline{\varphi^+(y)} = \varphi^-(y) + \overline{\varphi^-(y)} = 0$. Splitting φ into a
86 symmetric and antisymmetric part as $\Omega(\zeta) = [\varphi(\zeta) + \overline{\varphi(\bar{\zeta})}]/2$ and $\Psi(\zeta) = [\varphi(\zeta) - \overline{\varphi(\bar{\zeta})}]/2$, it is then
87 straightforward to show that Ψ is analytic in the entire ζ plane, while Ω satisfies the homogeneous
88 Hilbert problem

$$\Omega^+(y) + \Omega^-(y) = 0$$

89 on the positive half of the real axis. Requiring an integrable heat flux φ' , we have a general solution

$$\varphi(\zeta) = \Omega(\zeta) + \Psi(\zeta) = -\zeta^{1/2} \sum_{n=0}^{\infty} \frac{ia_n}{2} \zeta^n - \sum_{n=0}^{\infty} \frac{ib_n}{2} \zeta^n$$

90 where $\zeta^{1/2}$ has a branch cut on the positive half of the real axis, the limit taken from above being the
91 usual positive square root \sqrt{y} , and the a_n and b_n are purely real to satisfy the symmetries of Ω and
92 Ψ .

93 To an error of $O(r^{5/2})$, we therefore obtain a temperature field close to the origin of the form

$$\begin{aligned}
T(r, \vartheta) = & \frac{\tau_c^2}{4\pi^2 k \eta} r^2 \left\{ \left[\left(\log \left(\frac{r}{r_0} \right) - 1 \right)^2 + \vartheta^2 \right] - \cos(2\vartheta) \left[\left(\log \left(\frac{r}{r_0} \right) - 1 \right)^2 - \vartheta^2 \right] \right. \\
& + 2(\vartheta - \pi) \sin(2\vartheta) \left(\log \left(\frac{r}{r_0} \right) - 1 \right) - \pi \sin(2\vartheta) - 2\pi\vartheta \cos(2\vartheta) \left. \right\} - \frac{\tau_c \bar{u}_b}{k} r \sin(\vartheta) \\
& + a_0 r^{1/2} \sin \left(\frac{\vartheta}{2} \right) + a_1 r^{3/2} \sin \left(\frac{3\vartheta}{2} \right) + b_1 r \sin(\vartheta) + b_2 r^2 \sin(2\vartheta)
\end{aligned}$$

94 for $0 < \vartheta < \pi$, and

$$T(r, \vartheta) = a_0 r^{1/2} \sin \left(\frac{\vartheta}{2} \right) + a_1 r^{3/2} \sin \left(\frac{3\vartheta}{2} \right) + b_1 r \sin(\vartheta) + b_2 r^2 \sin(2\vartheta)$$

95 for $\pi < \vartheta < 2\pi$. The response to englacial shear heating is represented by the term in curly brackets,
96 which behaves as $O(r^2 \log(r)^2)$. The temperature is therefore dominated by the terms in the solution
97 to the problem without englacial heating, of the form

$$T \sim a_0 r^{1/2} \sin(\vartheta/2) + a_1 r^{3/2} \sin(3\vartheta/2) + b_1 r \sin(\vartheta) + b_2 r^2 \sin(2\vartheta) - \begin{cases} \frac{\tau_c \bar{u}_b}{k} r \sin(\vartheta) & \text{for } 0 < \vartheta < \pi \\ 0 & \text{otherwise.} \end{cases}$$

98 As in Schoof (2012), it is easy to see that we require $a_0 \leq 0$ to ensure temperatures do not go above
99 freezing at the bed on the cold side of the transition point (that is, on $\vartheta = \pi$, where the leading order
100 form of T is then $T \sim a_0 r^{1/2}$). A consequence of this is that, with $a_0 \neq 0$, we obtain a singular heat
101 flux $-kr^{-1} \partial T / \partial \vartheta|_{\vartheta=2\pi}^{\vartheta=0} = ka_0 r^{-1/2}$ out of the bed on the warm side.

102 If we assume that a singular heat flux out of the bed is not viable as it leads to freezing of the
103 bed on the warm side of the transition, contradicting the assumption that the ice stream is widening,

104 then we must have $a_0 = 0$. The temperature field near the origin is then linear at leading order, and
 105 can be written as $T \sim b_1 z$ for $z < 0$, $T \sim [b_1 - \tau_c \bar{u}_b/k]z$ for $z > 0$, with the horizontal temperature
 106 gradient only appearing at the next (higher) order.

107 There are two important conclusions that can be drawn from this. The first is that the net heat
 108 flux out of the bed is

$$-\frac{1}{r} \frac{\partial T}{\partial \vartheta} \Big|_{2\pi}^0 = -\frac{1}{r} \frac{\partial T}{\partial \vartheta} \Big|_{\pi^+}^{\pi^-} = \tau_c \bar{u}$$

109 on both, the cold and the warm sides of the transition: it is impossible for the temperature gradient
 110 to change discontinuously from the left to the right of the transition point. The fact that the frictional
 111 heat $\tau_c \bar{u}_b$ generated to the left of the transition must be removed from the bed means that heat is
 112 removed at the same rate from the right, where presumably it must be supplied in the form of latent
 113 heat transported by drainage of meltwater along the bed. The second observation is that it is no
 114 longer necessary to have a region of temperate ice form near the transition point: if the temperature
 115 below the bed is above the melting point, we expect $b_1 < 0$ and hence $\partial T/\partial z < 0$ everywhere above
 116 the bed, corresponding to temperatures below the melting point in the ice.

117 **S3 The velocity field close to the transition from no slip to free slip**

118 In section 4.3 we analyze the behavior of the temperature field close to the transition from no slip
 119 to free slip. To do so, we need to know the behavior of the velocities close to the origin, which we
 120 consider here. Near the origin of our geometry, i.e. for $R = (Y^2 + Z^2)^{1/2} \rightarrow 0$ and for $\varepsilon \ll 1$, the
 121 equation for the down-stream velocity (22) with boundary conditions (29)–(30a) is identical to the
 122 model for a crack-tip considered in Rice (1967, 1968). He shows that in polar coordinates, the velocity
 123 solution close to the transition from free slip to no slip is of the form

$$U \sim C_u R^{\frac{1}{n+1}} \sqrt{\frac{2n}{n+1} A_\vartheta^{\frac{2}{n+1}} + \cos \vartheta A_\vartheta^{\frac{1-n}{1+n}}} \quad \text{for } R \rightarrow 0, \quad (\text{S7})$$

124 where $R = \sqrt{Y^2 + Z^2}$, $\cos \vartheta = Y/R$, C_u a constant that depends on the far field conditions, and

$$A_\vartheta = \frac{n^2 - 1}{4n} \cos \vartheta + \sqrt{\left(\frac{n^2 - 1}{4n}\right)^2 \cos^2 \vartheta + \frac{(n+1)^2}{4n}}. \quad (\text{S8})$$

125 Figures S2a and S3a confirm that our numerical solution reproduces this behavior as $R \rightarrow 0$. From
 126 (S7) the asymptotic behavior of the heat production rate (32) is

$$\mathcal{A} \sim \left(\frac{C_u}{2}\right)^{1+1/n} R^{-1} A_\vartheta^{-1}. \quad (\text{S9})$$

127 The important feature of this result is that the heat production is singular, behaving as R^{-1} near the
 128 transition point. This is not a surprise: a similar behavior for $n = 1$ appears in Schoof (2004, 2012)
 129 and for $n = 3$ in Suckale et al. (2014). For the frequently used special cases of $n = 1$ and $n = 3$, \mathcal{A}
 130 can alternatively be written as

$$\mathcal{A} \sim C_a R^{-1} \times \begin{cases} \text{const.} & \text{for } n = 1, \\ \left(\sqrt{3 + \cos^2 \vartheta} + \cos \vartheta\right)^{-1} & \text{for } n = 3. \end{cases} \quad (\text{S10})$$

131 The local behavior of the across-stream velocities (V, W) is more difficult to determine. For a
 132 constant viscosity ($n = 1$), Barcilon and MacAyeal (1993) show that

$$V \sim C_v R^{1/2} \left(11 \cos \frac{\vartheta}{2} - \cos \frac{3\vartheta}{2}\right), \quad W \sim -C_w R^{1/2} \left(\sin \frac{\vartheta}{2} + \sin \frac{3\vartheta}{2}\right). \quad (\text{S11})$$

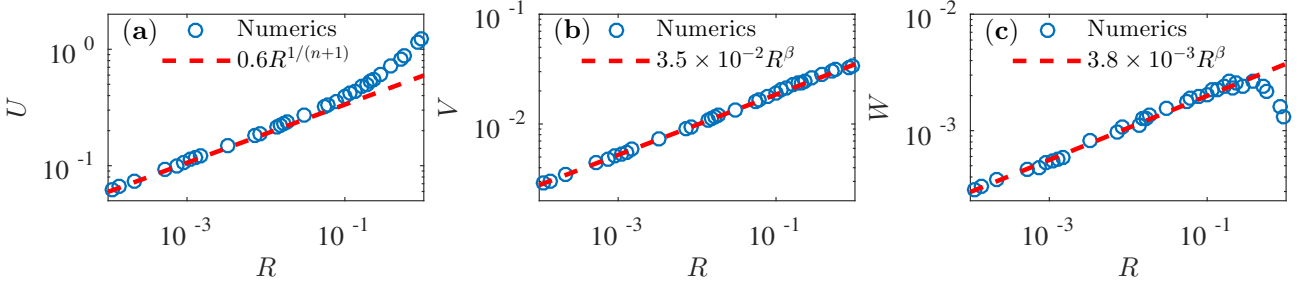


Figure S2: Comparison of numerical velocity solutions with asymptotic solutions from Rice (1967) and the solutions of the boundary value problem (S18)–(S20) for $\vartheta = \pi/8$. Panel a shows solutions of the downstream velocity U , panel b shows solutions of the across-stream velocity V and panel c shows solutions of the vertical velocity W . $n = 3$ in all three cases.

133 For $n \neq 1$, the problem of finding the local behavior of V and W is complicated by the fact that the
 134 viscosity is determined by $|\nabla U|$, where the local behavior of U is given by (S7). To find a generalization
 135 of (S11) for $n \neq 1$, we rewrite (23) in polar coordinates (R, ϑ) :

$$-\frac{\partial P}{\partial R} + \frac{1}{R} \frac{\partial}{\partial R} (R \Sigma_{RR}) + \frac{1}{R} \frac{\partial \Sigma_{\vartheta R}}{\partial \vartheta} - \frac{\Sigma_{\vartheta \vartheta}}{R} = 0, \quad (\text{S12a})$$

$$-\frac{1}{R} \frac{\partial P}{\partial \vartheta} + \frac{1}{R^2} \frac{\partial}{\partial R} (R^2 \Sigma_{\vartheta R}) + \frac{1}{R} \frac{\partial \Sigma_{\vartheta \vartheta}}{\partial \vartheta} = 0, \quad (\text{S12b})$$

$$\frac{1}{R} \frac{\partial}{\partial R} (R V_R) + \frac{1}{R} \frac{\partial V_\vartheta}{\partial \vartheta} = 0. \quad (\text{S12c})$$

Here V_R and V_ϑ are the radial and angular velocity components, respectively, i.e., $\mathbf{V} = V_R \mathbf{e}_R + V_\vartheta \mathbf{e}_\vartheta$. The constitutive relations for the stresses Σ in polar coordinates are:

$$\Sigma_{RR} = \mu \frac{\partial V_R}{\partial R}, \quad \Sigma_{\vartheta \vartheta} = \mu \frac{1}{R} \left(\frac{\partial V_\vartheta}{\partial \vartheta} + V_R \right), \quad \Sigma_{\vartheta R} = \frac{1}{2} \mu \left(\frac{1}{R} \frac{\partial V_R}{\partial \vartheta} + \frac{\partial v_\vartheta}{\partial R} - \frac{v_\vartheta}{R} \right).$$

136 The boundary conditions (29) and (30a) at the base become

$$V_\vartheta = \mu \frac{1}{R} \frac{\partial V_R}{\partial \vartheta} = 0 \quad \text{for } \vartheta = 0, \quad V_\vartheta = V_R = 0 \quad \text{for } \vartheta = \pi. \quad (\text{S13})$$

137 The downstream velocity U , given by (S7)–(S8) determines the viscosity μ through

$$\mu \sim R^{\frac{1-n}{1+n}} N \quad \text{with} \quad N(\vartheta) = [A_\vartheta(\vartheta)]^{\frac{n-1}{n+1}}. \quad (\text{S14})$$

138 We put $\mu = R^{\frac{1-n}{1+n}} N$ and make the *ansatz* $(V_R, V_\vartheta) = R^\beta (\bar{V}_R(\vartheta), \bar{V}_\vartheta(\vartheta))$ and $P = R^{\beta-2/(n+1)} P_\vartheta(\vartheta)$,
 139 which gives in (S12c)

$$\bar{V}_R + \frac{1}{\beta+1} \bar{V}_\vartheta' = 0. \quad (\text{S15})$$

140 Here a prime denotes an ordinary derivative with respect to ϑ , so $\bar{V}_\vartheta' = d\bar{V}_\vartheta/d\vartheta$. Equations (S12a)–
 141 (S12b) become

$$-a_0 P_\vartheta - a_1 N \bar{V}_\vartheta' + (a_2 N \bar{V}_\vartheta - a_3 N \bar{V}_\vartheta'')' = 0, \quad (\text{S16a})$$

$$-P_\vartheta' + b_1 N \bar{V}_\vartheta - b_2 N \bar{V}_\vartheta'' + b_3 (N' \bar{V}_\vartheta' + N \bar{V}_\vartheta'') = 0, \quad (\text{S16b})$$

142 where

$$a_0 = \left[\beta - \frac{2}{n+1} \right], \quad a_1 = \frac{\beta}{\beta+1} \left[\beta + \frac{2n}{n+1} \right], \quad a_2 = \frac{(\beta-1)}{2}, \quad a_3 = \frac{1}{2} \frac{1}{\beta+1},$$

$$b_1 = \frac{1}{2} \left(\beta + \frac{2n}{n+1} \right) (\beta-1), \quad b_2 = \frac{1}{2} \left(\beta + \frac{2n}{n+1} \right) \frac{1}{\beta+1}, \quad b_3 = \frac{\beta}{\beta+1}.$$

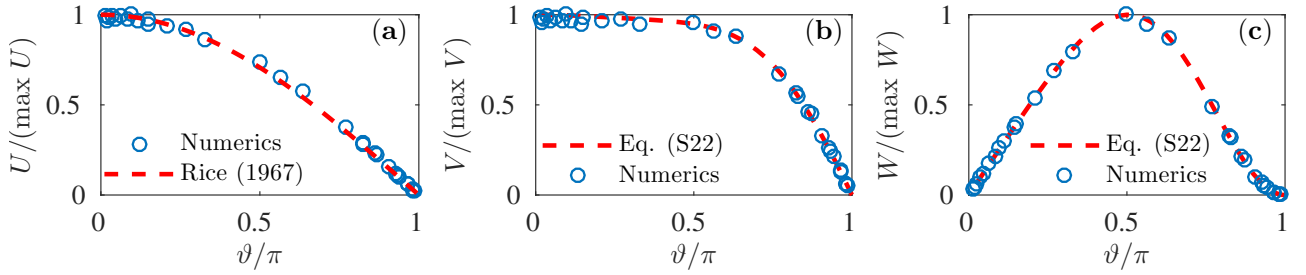


Figure S3: Comparison of numerical velocity solutions with asymptotic solutions from Rice (1967) and the solutions of the boundary value problem (S18)–(S20) for $R = 0.01$. Panel a shows scaled solutions of the downstream velocity U , panel b shows scaled solutions of the across-stream velocity V and panel c shows solutions of the vertical velocity W . $n = 3$ in all three cases.

143

144 Elimination of the pressure in (S16a) by use of (S16b) leads to a fourth order homogeneous differ-
 145 ential equation for \bar{V}_ϑ with non-constant coefficients

$$0 = \left(b_1 + c_5 \frac{N''}{N} \right) \bar{V}_\vartheta + \left(c_4 \frac{N'}{N} - c_2 \right) \bar{V}_\vartheta' + \left(c_3 - \frac{N''}{N} \right) \bar{V}_\vartheta'' - 2 \frac{N'}{N} \bar{V}_\vartheta''' - \bar{V}_\vartheta'''' \quad (\text{S18})$$

146 where

$$c_1 = \frac{a_0}{a_3} b_1, \quad c_2 = \frac{a_1}{a_3}, \quad c_3 = \frac{a_0}{a_3} (b_2 - b_3) + \frac{a_2}{a_3}, \quad c_4 = \left[2 \frac{a_2}{a_3} - \frac{a_1}{a_3} - \frac{a_0}{a_3} b_3 \right], \quad c_5 = \frac{a_2}{a_3}, \quad (\text{S19})$$

147 and N is given by equation (S14). The boundary conditions (S13) are likewise homogeneous,

$$\bar{V}_\vartheta = \bar{V}_\vartheta'' = 0 \quad \text{for } \vartheta = 0, \quad \bar{V}_\vartheta = \bar{V}_\vartheta' = 0 \quad \text{for } \vartheta = \pi, \quad (\text{S20})$$

148 and we have a generalized eigenvalue problem in which the eigenvalue β is somewhat unconventionally
 149 hidden in the coefficients (S19). We solve this problem using a shooting method, which gives $\beta =$
 150 $0.271\dots$ as the lowest positive eigenvalue for $n = 3$. Once again we find that our numerical solutions
 151 reproduce this behavior, see figure S2b-c. Note that β is greater than $1/(1+n)$, so that the viscosity
 152 is indeed dominated by gradients of the downstream velocity U . The shooting method also gives us
 153 \bar{V}_ϑ , from which \bar{V}_R can be calculated through equation (S15). The velocity components (V, W) in
 154 Cartesian coordinates can be calculated from $(\bar{V}_R, \bar{V}_\vartheta)$ through

$$V = R^\beta (\bar{V}_R \cos \vartheta - \bar{V}_\vartheta \sin \vartheta), \quad W = R^\beta (\bar{V}_R \sin \vartheta + \bar{V}_\vartheta \cos \vartheta). \quad (\text{S21})$$

155 The angular dependence of U, V and W is shown in figure S3.

156 Note that the local solution we have derived here stems from a problem (equations (22)–(30b) of
 157 the main text) that contains no free parameters when — as we have assumed here — τ is infinite. As
 158 a result, we are guaranteed that C_a, C_u, \bar{V}_R and \bar{V}_ϑ are also parameter-free, as is implied in the main
 159 text.

160 S4 The outer temperature problem for strong heat production

161 In the main text, the velocity field derived in section S3 above is used to construct a local advection-
 162 diffusion problem for heat transport near the cold-temperate (and no-slip-to-slip) transition. That
 163 local model, equations (40) of the main text, is mathematically a boundary layer. It only depends on
 164 Λ and \tilde{V}_m as parameters, suggesting that $\tilde{V}_m = \tilde{f}(\Lambda)$, if the far-field conditions on the boundary layer
 165 only depend on Λ , too. These boundary conditions mathematically come out of asymptotic matching
 166 with an ‘outer’ problem that describes heat transport at a larger scale (Holmes, 2013). Here we verify
 167 that matching leads to far-field conditions that only depend on Λ as required.

168 The outer problem to the conductive boundary layer itself describes heat flow in a slender region
 169 along the bed. To identify leading order terms in this outer problem (confusingly, itself a boundary
 170 layer to the advection-dominated heat transport across the bulk of the ice thickness), we first need
 171 to understand the transverse velocity field near the bed. $V = 0$ implies that $\partial V/\partial Y = 0$ at the
 172 bed, so $\partial W/\partial Z = 0$ by mass conservation. By Taylor expansion, we obtain $V \sim Z$, $W \sim Z^2$.
 173 Near-bed advection in the outer problem is captured by considering a thin region of vertical extent
 174 $Z_{\text{Pe}} = \text{Pe}^{-\beta/(1+\beta)} \ll 1$ relative to ice thickness, labeled the ‘advective boundary layer’ in figure 5.
 175 Within this region, we rescale $Z = Z_{\text{Pe}}\widehat{Z}$, $V = Z_{\text{Pe}}\widehat{V}$, $W = Z_{\text{Pe}}^2\widehat{W}$, $\mathcal{A} = \widehat{\mathcal{A}}$, $\Theta = \widehat{\Theta}$.

176 Note that the vertical coordinate in the advective region is related to the vertical coordinate in
 177 the conductive boundary layer through $\widetilde{Z} = \Lambda^{-1}\text{Pe}^{(1-\beta)/(1+\beta)}\widehat{Z}$. For $\beta < 1$, $\widehat{Z} = O(1)$ implies that
 178 $\widetilde{Z} \gg 1$. For $n = 1$, the exponent β equals $1/2$, and for $n = 3$ we have $\beta \approx 0.27$ (see supplementary
 179 section S3). Therefore the near-bed advective layer is a viable outer region to the conductive boundary
 180 layer because the advective layer has a much larger vertical and horizontal extent than the conductive
 181 boundary layer.

182 For $n = 3$ (or generally for $n > 1$ and $\beta < 1/2$), the outer problem is,

$$\widetilde{V}_m \frac{\partial \widehat{\Theta}}{\partial \widehat{Y}} + \Lambda \left(\widehat{V} \frac{\partial \widehat{\Theta}}{\partial \widehat{Y}} + \widehat{W} \frac{\partial \widehat{\Theta}}{\partial \widehat{Z}} \right) = a \quad \text{for } 0 < \widehat{Z}, \quad (\text{S22a})$$

$$\widetilde{V}_m \frac{\partial \widehat{\Theta}}{\partial \widehat{Y}} = 0 \quad \text{for } \widehat{Z} < 0, \quad (\text{S22b})$$

183 to an error of $O(\text{Pe}^{(2\beta-1)/(1+\beta)})$. As required, (S22a)–(S22b) only depend on \widetilde{V}_m and Λ . As we are
 184 considering an outer problem that describes a slender region near the bed, our choice of reduced
 185 temperature Θ means that the relevant boundary condition is $\widehat{\Theta}(\widehat{Z} = 0) \rightarrow 0$ as $Y \rightarrow -\infty$, equation
 186 (34c), which equally does not depend on any additional parameters.

187 S5 Mechanical problem for a small slip region: $\tau \sim \alpha^{1/(n+1)} \gg 1$

188 When we allow for subtemperate sliding, but at a large basal yield stress $\tau \gg 1$, the velocity field will
 189 change only by a small amount: over most of the domain, basal shear stress will not attain the yield
 190 stress. The only location where that is not the case is close to the origin, where a hard transition from
 191 slip to no slip would lead to a stress singularity, exceeding any finite yield stress. In other words, the
 192 region of slip created by a large but finite τ is a mechanical boundary layer close to the origin, which
 193 remains small compared with the ice thickness. Outside that boundary layer, the velocity field will
 194 remain unchanged. In fact, at length scales that are intermediate between the boundary layer and the
 195 ice thickness scales, the local solution of supplementary section S4 will still apply, and provides the
 196 appropriate matching conditions on the mechanical boundary layer created by the small slip region.
 197 In this section, we construct a leading order model for that boundary layer. We focus on the case
 198 of $\tau \sim \alpha^{1/(n+1)} \gg 1$, in which the size of this mechanical boundary layer is the same as the size of
 199 the thermal boundary layer: this is the minimum size of the mechanical boundary layer at which we
 200 expect to start seeing an effect of subtemperate sliding on margin migration.

201 We rescale the mechanical field equations using $(Y, Z) = R_\alpha(\widetilde{Y}, \widetilde{Z})$, $\mathcal{A} = R_\alpha^{-1}\widetilde{\mathcal{A}}$, $U = R_\alpha^{1/(n+1)}\widetilde{U}$,
 202 $(V, W) = R_\alpha^\beta(\widetilde{V}, \widetilde{W})$, and $P = R_\alpha^{-1/(n+1)}\widetilde{P}$ where $R_\alpha = \alpha^{-1}$. The choice of exponent β ensures that
 203 the boundary layer solution can be matched with the outer problem at the ice thickness scale, whose
 204 behavior in the matching region (Holmes, 2013) is given by supplementary section S4 as discussed.
 205 This yields an equation for the velocity in the downstream direction of the same form as (22):

$$\frac{\partial}{\partial \widetilde{Y}} \left(\widetilde{\mu} \frac{\partial \widetilde{U}}{\partial \widetilde{Y}} \right) + \frac{\partial}{\partial \widetilde{Z}} \left(\widetilde{\mu} \frac{\partial \widetilde{U}}{\partial \widetilde{Z}} \right) = 0. \quad (\text{S23})$$

206 In the across-stream direction, we obtain from (23)

$$\frac{\partial}{\partial \tilde{Y}} \left(2\tilde{\mu} \frac{\partial \tilde{V}}{\partial \tilde{Y}} \right) + \frac{\partial}{\partial \tilde{Z}} \left[\tilde{\mu} \left(\frac{\partial \tilde{V}}{\partial \tilde{Z}} + \frac{\partial \tilde{W}}{\partial \tilde{Y}} \right) \right] - \frac{\partial \tilde{P}}{\partial \tilde{Y}} = 0, \quad (\text{S24a})$$

$$\frac{\partial}{\partial \tilde{Y}} \left[\tilde{\mu} \left(\frac{\partial \tilde{V}}{\partial \tilde{Z}} + \frac{\partial \tilde{W}}{\partial \tilde{Y}} \right) \right] + \frac{\partial}{\partial \tilde{Z}} \left(2\tilde{\mu} \frac{\partial \tilde{W}}{\partial \tilde{Z}} \right) - \frac{\partial \tilde{P}}{\partial \tilde{Z}} = 0, \quad (\text{S24b})$$

$$\frac{\partial \tilde{V}}{\partial \tilde{Y}} + \frac{\partial \tilde{W}}{\partial \tilde{Z}} = 0. \quad (\text{S24c})$$

207 μ is the rescaled non-dimensional viscosity

$$\tilde{\mu} = \frac{1}{2^{1/n}} \left[\left| \frac{\partial \tilde{U}}{\partial \tilde{Y}} \right|^2 + \left| \frac{\partial \tilde{U}}{\partial \tilde{Z}} \right|^2 \right]^{\frac{1-n}{2n}}. \quad (\text{S25})$$

208 As before, we find for the vertical velocity component along the bed

$$\tilde{W} = 0 \quad \text{at} \quad \tilde{Z} = 0. \quad (\text{S26})$$

209 Similarly, the free slip boundary condition (29) on the temperate side remains unchanged

$$\tilde{\mu} \frac{\partial \tilde{U}}{\partial \tilde{Z}} = \tilde{\mu} \frac{\partial \tilde{V}}{\partial \tilde{Z}} = 0 \quad \text{at} \quad \tilde{Z} = 0, \quad \tilde{Y} > 0. \quad (\text{S27})$$

210 On the frozen side of the bed, we have from (30b)

$$\left. \begin{array}{l} \text{either} \quad \tilde{\mu} \frac{\partial \tilde{U}}{\partial \tilde{Z}} = \alpha^{1/(n+1)} \tau \frac{\tilde{U}}{|\tilde{U}|}, \quad \tilde{\mu} \frac{\partial \tilde{V}}{\partial \tilde{Z}} = \alpha^{1/(n+1)} \tau \frac{\tilde{V}}{|\tilde{V}|}, \quad |\tilde{U}| > 0, \quad |\tilde{V}| > 0 \\ \text{or} \quad \left| \tilde{\mu} \frac{\partial \tilde{U}}{\partial \tilde{Z}} \right| < \alpha^{1/(n+1)} \tau, \quad \left| \tilde{\mu} \frac{\partial \tilde{V}}{\partial \tilde{Z}} \right| < \alpha^{1/(n+1)} \tau \left| \frac{\tilde{V}}{\tilde{U}} \right|, \quad |\tilde{U}| = |\tilde{V}| = 0 \end{array} \right\} \text{for } \tilde{Y} < 0, \quad \tilde{Z} = 0. \quad (\text{S28})$$

211 Equations (S23)–(S28) only depend on $\alpha^{1/(n+1)} \tau = \Gamma^{-(n+1)}$, as required for (46) to hold.

212 **S6 Limit of large slip region:** $\tau_c \ll \tau_s$

213 We conclude by considering the opposite parametric limit in τ to that considered above: we derive
 214 an otherwise elusive closed-form expression for V_m in the limit $\tau \ll 1$. When considering the case of
 215 small basal yield stress τ , the region of subtemperate slip becomes wide compared with ice thickness.
 216 Simultaneously, we consider the case of $\alpha \gg 1$, $\text{Pe} \gg 1$, identifying the relevant distinguished limit as
 217 $\tau \text{Pe} \sim \alpha^2 \gg 1$ later.

218 There are two rescalings required: first, for the mechanical problem and second, for the thermal
 219 problem. For the mechanical problem, we put

$$\hat{Y} = \tau Y, \quad \hat{Z} = Z, \quad \hat{U} = \tau U, \quad \hat{V} = V, \quad \hat{W} = \tau^{-1} W, \quad \hat{P} = \tau^{-1} P. \quad (\text{S29})$$

220 Under this rescaling, the mechanical problem in the boundary layer becomes

$$\tau^2 \frac{\partial}{\partial \hat{Y}} \left(\hat{\mu} \frac{\partial \hat{U}}{\partial \hat{Y}} \right) + \frac{\partial}{\partial \hat{Z}} \left(\hat{\mu} \frac{\partial \hat{U}}{\partial \hat{Z}} \right) = 0, \quad (\text{S30a})$$

$$\tau^2 \frac{\partial}{\partial \hat{Y}} \left(2\hat{\mu} \frac{\partial \hat{V}}{\partial \hat{Y}} \right) + \frac{\partial}{\partial \hat{Z}} \left[\hat{\mu} \left(\frac{\partial \hat{V}}{\partial \hat{Z}} + \tau^2 \frac{\partial \hat{W}}{\partial \hat{Y}} \right) \right] - \tau^2 \frac{\partial \hat{P}}{\partial \hat{Y}} = 0, \quad (\text{S30b})$$

$$\frac{\partial}{\partial \hat{Y}} \left[\hat{\mu} \left(\frac{\partial \hat{V}}{\partial \hat{Z}} + \tau^2 \frac{\partial \hat{W}}{\partial \hat{Y}} \right) \right] + \frac{\partial}{\partial \hat{Z}} \left(2\hat{\mu} \frac{\partial \hat{W}}{\partial \hat{Z}} \right) - \frac{\partial \hat{P}}{\partial \hat{Z}} = 0, \quad (\text{S30c})$$

$$\frac{\partial \hat{V}}{\partial \hat{Y}} + \frac{\partial \hat{W}}{\partial \hat{Z}} = 0, \quad (\text{S30d})$$

221 where

$$\hat{\mu} = \frac{1}{2^{1/n}} \left[\left(\frac{\partial \hat{U}}{\partial \hat{Y}} \right)^2 + \tau^{-2} \left(\frac{\partial \hat{U}}{\partial \hat{Z}} \right)^2 \right]^{(1-n)/(2n)} \quad (\text{S31})$$

222 for $0 < \hat{Z} < 1$. Assume that there is slip for $\hat{Y}_0 < \hat{Y} < 0$, meaning $\hat{U} > 0$ at $\hat{Z} = 0$. In that region, we
 223 then have the following boundary conditions

$$\hat{\mu} \frac{\partial \hat{U}}{\partial \hat{Z}} = 0, \quad \hat{\mu} \left(\frac{\partial \hat{V}}{\partial \hat{Z}} + \tau^2 \frac{\partial \hat{W}}{\partial \hat{Y}} \right) = 0, \quad \hat{W} = 0 \quad \text{for } \hat{Y} > 0, \hat{Z} = 0, \quad (\text{S32a})$$

$$\hat{\mu} \frac{\partial \hat{U}}{\partial \hat{Z}} = \tau^2, \quad \hat{\mu} \left(\frac{\partial \hat{V}}{\partial \hat{Z}} + \tau^2 \frac{\partial \hat{W}}{\partial \hat{Y}} \right) = \tau^2 \frac{\hat{V}}{\hat{U}}, \quad \hat{W} = 0 \quad \text{for } \hat{Y}_0 < \hat{Y} < 0, \hat{Z} = 0. \quad (\text{S32b})$$

224 Expanding as $\hat{U} = \hat{U}^{(0)} + \tau^2 \hat{U}^{(1)} + \dots$, $\hat{V} = \hat{V}^{(0)} + \tau^2 \hat{V}^{(1)} + \dots$, $\hat{W} = \hat{W}^{(0)} + \tau^2 \hat{W}^{(1)} + \dots$, we find
 225 that $\hat{U}^{(0)} = \hat{U}^{(0)}(\hat{Y})$, $\hat{V}^{(0)} = \text{constant}$, $\hat{W}^{(0)} = 0$. In other words, a wide region of subtemperate slip
 226 implies that the plug flow of the ice stream extends past the thermal margin of the ice stream into a
 227 rapidly sliding but cold-based region. The axial velocity $\hat{U}^{(0)}$ here satisfies the ice-stream-like model
 228 for a laterally sheared plug flow with constant basal drag:

$$\frac{\partial}{\partial \hat{Y}} \left(\frac{1}{2^{1/n}} \left| \frac{\partial \hat{U}^{(0)}}{\partial \hat{Y}} \right|^{(1-n)/n} \frac{\partial \hat{U}^{(0)}}{\partial \hat{Y}} \right) - 1 = 0$$

229 for the region $\hat{Y}_0 < \hat{Y} < 0$ where $\hat{U}^{(0)} > 0$ (this can be shown by vertical integration of (S30a), bearing
 230 in mind that $\hat{\mu} \partial \hat{U} / \partial \hat{Z} = 0$ at the ice stream surface at $\hat{Z} = 1$, (27)). On the ice stream side $\hat{Y} > 0$,
 231 we have no basal drag and so the equivalent model is

$$\frac{\partial}{\partial \hat{Y}} \left(\frac{1}{2^{1/n}} \left| \frac{\partial \hat{U}^{(0)}}{\partial \hat{Y}} \right|^{(1-n)/n} \frac{\partial \hat{U}^{(0)}}{\partial \hat{Y}} \right) = 0.$$

232 The original matching conditions with the ice stream as $Y \rightarrow \infty$ (25)₁ can then simply be reduced to
 233 a stress condition at $\hat{Y} = 0$,

$$\frac{1}{2^{1/n}} \left| \frac{\partial \hat{U}^{(0)}}{\partial \hat{Y}} \right|^{(1-n)/n} \frac{\partial \hat{U}^{(0)}}{\partial \hat{Y}} = 1 \quad \text{at } \hat{Y} = 0.$$

234 From (S30b) with (S32a)₂/(S32b)₂, we can see that the across-stream velocity $\hat{V}^{(0)}$ has no vertical
 235 profile, either. Vertically integrating the mass balance equation (S30d) with (S32a)₃ and (S32b)₃ and
 236 (27), we can further show $\partial \hat{V}^{(0)} / \partial \hat{Y} = 0$, or $\hat{V}^{(0)} = \text{constant}$.

237 Matching with the region $\hat{Y} < \hat{Y}_0$, where there is no sliding, in principle requires a boundary layer
 238 around $\hat{Y} < \hat{Y}_0$ whose extent is comparable with ice thickness. The appropriate rescaling in that
 239 boundary layer is

$$\check{Y} = Y - \tau^{-1} \hat{Y}_0, \quad \check{Z} = Z, \quad \check{U} = \tau^{-1} U, \quad \check{V} = V, \quad \check{W} = W, \quad \check{P} = P. \quad (\text{S33})$$

240 We do not give full detail of that boundary layer; the result of matching with (S30) and the far field
 241 as $\check{Y} \rightarrow -\infty$ is simply the intuitive result that

$$\hat{U}^{(0)} = \frac{\partial \hat{U}^{(0)}}{\partial \hat{Y}} = 0, \quad \hat{V}^{(0)} = \int_0^1 1 - (1 - \hat{Z})^{n+1} d\hat{Z} = \frac{n+1}{n+2} \quad \text{at } \hat{Y} = \hat{Y}_0,$$

242 and we have a solution for the sliding velocity of the form

$$\hat{U}^{(0)} = \frac{2(\hat{Y} - \hat{Y}_0)^{n+1}}{n+1},$$

243 with

$$\widehat{Y}_0 = -1.$$

244 Putting $\widehat{T} = \mathcal{T}$, the corresponding thermal problem in the region with subtemperate slip is then
 245 at leading order in τ^2

$$\tau V_m \frac{\partial \widehat{T}}{\partial \widehat{Y}} + \text{Pe}\tau \widehat{V}^{(0)} \frac{\partial \widehat{T}}{\partial \widehat{Y}} - \frac{\partial^2 \widehat{T}}{\partial \widehat{Z}^2} = \frac{\alpha}{2^{1+1/n}} \left| \frac{\partial \widehat{U}}{\partial \widehat{Y}} \right|^{n+1} \quad \text{for } 0 < \widehat{Z} < 1, \quad (\text{S34a})$$

$$\gamma \tau V_m \frac{\partial \widehat{T}}{\partial \widehat{Y}} - \kappa \frac{\partial^2 \widehat{T}}{\partial \widehat{Z}^2} = 0 \quad \text{for } \widehat{Z} < 0 \quad (\text{S34b})$$

246 subject to the jump conditions

$$\left[\widehat{T} \right]_{-}^{+} = 0, \quad - \left. \frac{\partial \widehat{T}}{\partial \widehat{Z}} \right|^{+} + \kappa \left. \frac{\partial \widehat{T}}{\partial \widehat{Z}} \right|^{-} = \alpha \widehat{U}^{(0)} \quad \text{at } \widehat{Z} = 0, \quad \widehat{Y}_0 < \widehat{Y} < 0. \quad (\text{S34c})$$

247 As before, we assume that $\alpha \gg 1$ and $\text{Pe} \gg 1$. With $\alpha \gg 1$, we require a short vertical length
 248 scale α^{-1} to be able to conduct heat generated at the bed through frictional sliding into the ice, and
 249 a commensurately large migration velocity to balance vertical conduction at that scale. If we assume
 250 that lateral inflow can also contribute to energy balance at the same scale, we require the distinguished
 251 limit

$$\text{Pe}\tau \sim \alpha^2$$

252 and can rescale as

$$\check{V}_m = \text{Pe}^{-1} V_m, \quad \check{Y} = \widehat{Y} - \widehat{Y}_0, \quad \check{Z} = \alpha \widehat{Z}, \quad \check{T} = \widehat{T} \quad (\text{S35})$$

253 leading to the leading order diffusive boundary layer problem

$$\frac{\text{Pe}\tau}{\alpha^2} \left(\widehat{V}^{(0)} + \check{V}_m \right) \frac{\partial \check{T}}{\partial \check{Y}} - \frac{\partial^2 \check{T}}{\partial \check{Z}^2} = 0 \quad \text{for } 0 < \check{Z} < 1, \quad (\text{S36a})$$

$$\gamma \frac{\text{Pe}\tau}{\alpha^2} \check{V}_m \frac{\partial \check{T}}{\partial \check{Y}} - \kappa \frac{\partial^2 \check{T}}{\partial \check{Z}^2} = 0 \quad \text{for } \check{Z} < 0, \quad (\text{S36b})$$

254 subject to the jump conditions

$$\left[\check{T} \right]_{-}^{+} = 0, \quad - \left. \frac{\partial \check{T}}{\partial \check{Z}} \right|^{+} + \kappa \left. \frac{\partial \check{T}}{\partial \check{Z}} \right|^{-} = \widehat{U}^{(0)} = \frac{2\check{Y}^{n+1}}{n+1} \quad \text{at } \check{Z} = 0. \quad (\text{S36c})$$

255 The outer problem in $\check{Z} = \alpha \widehat{Z}$ to this advection-diffusion boundary layer problem is simply the leading
 256 order (in $\alpha^2 \sim \text{Pe}\tau$) version of (S34), which is the pure advection problem

$$\frac{\text{Pe}\tau}{\alpha^2} \left(\widehat{V}^{(0)} + \check{V}_m \right) \frac{\partial \check{T}}{\partial \check{Y}} = 0 \quad \text{for } 0 < \check{Z} < 1, \quad (\text{S37a})$$

$$\gamma \frac{\text{Pe}\tau}{\alpha^2} \check{V}_m \frac{\partial \check{T}}{\partial \check{Y}} = 0 \quad \text{for } \check{Z} < 0, \quad (\text{S37b})$$

257 leading to the conclusion that, outside the diffusive boundary layer with height above or below the
 258 bed described by $\check{Z} \sim O(1)$, we simply have the far-field temperature field advected from $\check{Y} = 0$.

259 From the rescaling above, we can immediately see that we expect

$$V_m = \text{Pe} \check{V}_m = \frac{\alpha^2}{\tau} f \left(\frac{\text{Pe}\tau}{\alpha^2}, \gamma, \kappa \right)$$

260 for some function f (in fact, the dependence on κ and γ can be shown to collapse onto a dependence
 261 on the product $\kappa\gamma$ alone). It turns out we can compute the function f exactly, which we do below.

262 The boundary conditions (S36c) only hold up to $\check{Y} = -\widehat{Y}_0 = 1$. However, in the diffusion problem
 263 (S36), \check{Y} is the time-like variable (\check{Z} being space-like), and if we are only interested in the solution
 264 for $0 < \check{Y} < -\widehat{Y}_0$ (the region where subtemperate slip is possible), we can without loss of generality
 265 treat (S36) as applying for all $\check{Y} > 0$, which permits the problem to be solved by Laplace transforms.
 266 Define

$$\tilde{f}(s) = \mathcal{L}(f)(s) = \int_0^\infty f(\check{Y}) \exp(-s\check{Y}) d\check{Y}.$$

267 Then

$$\mathcal{L}(\check{Y}^{n+1}) = s^{-(n+2)}\Gamma(n+2)$$

268 where Γ is the standard gamma function. Let

$$\check{T} = \nu - 1 + \Theta,$$

269 so that (34c) becomes $\Theta = 0$ at $\check{Y} = 0$. Transforming (S36) gives

$$sv^\pm \tilde{\Theta} - \frac{\partial^2 \tilde{\Theta}}{\partial \check{Z}^2} = 0$$

270 with $v^+ = \text{Pe}\tau(\check{V}^{(0)} + \check{V}_m)/\alpha^2$ for $\check{Z} > 0$, $v^- = \gamma\text{Pe}\tau\check{V}_m/(\alpha^2\kappa)$ for $\check{Z} < 0$, and

$$\left[\tilde{\Theta} \right]_-^+ = 0, \quad - \left. \frac{\partial \tilde{\Theta}}{\partial \check{Z}} \right|_-^+ - \kappa \left. \frac{\partial \tilde{\Theta}}{\partial \check{Z}} \right|_-^- = \frac{2s^{-(n+2)}\Gamma(n+2)}{n+1} \quad \text{at } \check{Z} = 0.$$

271 Matching the outer problem additionally requires $\tilde{\Theta} \rightarrow 0$ as $\check{Z} \rightarrow \pm\infty$. This has solution

$$\tilde{\Theta} = A \exp\left(\mp\sqrt{sv^\pm}\check{Z}\right),$$

272 the upper sign being chosen consistently for $\check{Z} > 0$, the lower for $\check{Z} < 0$. The flux condition at $\check{Z} = 0$
 273 requires that

$$A\left(\sqrt{v^+s} + \kappa\sqrt{v^-s}\right) = \frac{2s^{-(n+2)}\Gamma(n+2)}{n+1}.$$

274 so that the Laplace transform of Θ at the bed is given by

$$\tilde{\Theta}\Big|_{\check{Z}=0} = A = \frac{2s^{-(n+5/2)}\Gamma(n+2)}{(n+1)\left(\sqrt{v^+} + \kappa\sqrt{v^-}\right)}.$$

275 We can now take the inverse Laplace transform; by inspection,

$$\Theta(\check{Y}, 0) = \frac{2\Gamma(n+2)}{(n+1)\Gamma(n+5/2)\left(\sqrt{v^+} + \kappa\sqrt{v^-}\right)} \check{Y}^{n+3/2}.$$

276 At $\check{Y} = -\widehat{Y}_0 = 1$, we must have temperature reaching the melting point $\check{T} = 0$, which becomes
 277 $\Theta = 1 - \nu$, so the migration velocity is determined by

$$\frac{2\Gamma(n+2)}{(n+1)\Gamma(n+5/2)\left(\sqrt{v^+} + \kappa\sqrt{v^-}\right)} = 1 - \nu,$$

278 or, using the definition of v^\pm ,

$$\frac{2\Gamma(n+2)}{(n+1)\Gamma(n+5/2)} \frac{\alpha}{(1-\nu)\sqrt{\text{Pe}\tau}} = \sqrt{\widehat{V}^{(0)} + \check{V}_m} + \sqrt{\kappa\gamma\check{V}_m}.$$

279 This is solvable in closed form; here we give only the (relatively simpler) solution for $\kappa\gamma = 1$, the case
 280 also considered in the main paper. Then, also recalling that $\check{V}_m = \text{Pe}^{-1}V_m$ and $\widehat{V}^{(0)} = (n+1)/(n+2)$,
 281 we can find the original migration velocity V_m as

$$V_m = \frac{\alpha^2}{\tau} \left[\frac{1}{n+1} \frac{\Gamma(n+2)}{\Gamma(n+\frac{5}{2})} - \frac{(n+1)^2}{4(n+2)} \frac{\Gamma(n+\frac{5}{2})}{\Gamma(n+2)} \frac{\text{Pe}\tau}{\alpha^2} \right]^2. \quad (\text{S38})$$

282 This formula is valid when the term in square brackets is non-negative (the term in square bracket
 283 being negative corresponds to insufficient heat production or too-rapid advection to cause widening
 284 of the ice stream).

285 References

- 286 Barcelon, V. and MacAyeal, D. R. (1993). Steady flow of a viscous ice stream across a no-slip/free-slip
 287 transition at the bed. *Journal of Glaciology*, 39:167–185.
- 288 England, A. (1971). *Complex Variable Methods in Elasticity*. J. Wiley & Sons, Ltd., London.
- 289 Haseloff, M. (2015). *Modelling the migration of ice stream margins*. PhD thesis, The University of
 290 British Columbia, Retrieved from <http://hdl.handle.net/2429/54268>.
- 291 Haseloff, M., Schoof, C., and Gagliardini, O. (2015). A boundary layer model for ice stream margins.
 292 *Journal of Fluid Mechanics*, 781:353–387.
- 293 Holmes, M. H. (2013). *Introduction to Perturbation Methods*. Springer New York.
- 294 Muskhelishvili, N. I. (1992). *Singular integral equations*. New York: Dover Publications, Inc.
 295 unabridged republication of 2nd edition published by P. Noordhoff, Groningen, 1953.
- 296 Rice, J. (1967). Stresses due to a sharp notch in a work-hardening elastic-plastic material loaded by
 297 longitudinal shear. *Journal of Applied Mechanics*, 34(2):287–298.
- 298 Rice, J. R. (1968). A path independent integral and the approximate analysis of strain concentration
 299 by notches and cracks. *Journal of Applied Mechanics*, 35(2):379–386.
- 300 Schoof, C. (2004). On the mechanics of ice-stream shear margins. *Journal of Glaciology*, 50:208–218.
- 301 Schoof, C. (2012). Thermally driven migration of ice-stream shear margins. *Journal of Fluid Mechan-*
 302 *ics*, 712:552–578.
- 303 Suckale, J., Platt, J. D., Perol, T., and Rice, J. R. (2014). Deformation-induced melting in the margins
 304 of the West Antarctic ice streams. *Journal of Geophysical Research*, 119:1004–1025.